

# Effect of the air cooled forced convection finned heat sinks on the TEG net power: experimental and simulation results

G. Montserrat<sup>1</sup>, I.R. Cózar<sup>1</sup>, L. Montoro<sup>1</sup>, A. Massaguer<sup>1</sup>, E. Massaguer<sup>2</sup>, M. Comamala<sup>1</sup> and T. Pujol<sup>1</sup>

<sup>1</sup> Department of Mechanical Engineering and Industrial Construction, EPS, University of Girona  
 Campus Montilivi, c\ Universitat de Girona 4, 17003 Girona (Spain)  
 Phone/Fax number: +0034 972 41 88 65 / +0034 972 41 80 98, e-mail: toni.pujol@udg.edu

<sup>2</sup> Nabla Thermoelectrics, c/ Llibertat 71, 17820, Banyoles (Spain)

**Abstract.** Thermoelectric generators (TEG) modules are devices that generate electrical power when there exists a temperature difference at its surfaces. The efficiency of TEGs depend on the ability to extract heat of its cold side. Some applications rely on air cooled forced convection finned heat sinks whose design parameters may greatly vary. Here we study the effects of the design parameters of finned heat sinks on the net output power. The net output power is equal to the power generated by the TEG minus the power absorbed by the fan that supplies air into the forced convection system. The analysis is carried out by means of computational fluid dynamics (CFD) simulations with the multi-physics commercial software ANSYS. The model has been validated with experimental data. Results show that, for a constant heat sink exchange area, a better performance is achieved with fin thicknesses greater than 1 mm.

## Key words

TEG, thermoelectric generator, forced convection, finned heat sink.

## 1. Introduction

Thermoelectric generators (TEGs) are junctions of type p- and n- semiconductors to which a heat flux is applied. These p- and n- legs are electrically connected in series and thermally in parallel. This generates electricity by means of the Seebeck effect [1].

Very recently, new advances in thermoelectric materials, with high values of figure of merit have boosted the research in this area. Thermoelectricity is assumed to be a very promising technique in the field of energy harvesting in waste heat applications, such as in exhaust gases of automobiles [2]. The fact that thermoelectric devices are free maintenance and do not contain mobile parts make them suitable solutions for several applications.

In low power applications, TEGs use simple air cooled heat sinks for enhancing the heat flow across it. In some cases, these air cooled finned heat sinks are adapted to

forced convection, so external fans are required in order to enhance the heat transfer. However, these fans absorb energy, which should be subtracted from that generated in order to get the net available power.

The purpose of the present paper is to analyse the effect of using different air cooled finned heat sinks on the net available power. The study is carried out with a numerical model that is validated with experimental data. Changes of fin thickness and fin to fin distances are evaluated in order to shed light into the effect of these parameters on the net available power of the complete power supply device (fan + TEG).

## 2. Experimental set up

The experimental set up consists in an open-circuit wind tunnel with a rectangular tube 500 mm long and with 40x40 mm cross-section (see Fig. 1). Two contraction cones guide the flow that finally reaches a 1 m long pipe of 150 mm inner diameter. At the end of this circular duct, a Hella 24V DC fan aspirates the flow through all the system. Honeycombs are inserted inside the two contraction cones in order to correctly redirect the flow.



Fig. 1. Experimental system.

The test zone is located at the middle of the rectangular zone, with a 41x41 mm rectangular hole in which the finned heat sink can be inserted. The tested one is aluminium made with 12 fins, 1.27 mm thick, and 36.80 mm high. The total height and length of the heat sink is 40x40 mm (see Fig. 2).

A thermoelectric generation module TEG 126-40B of EVERREDtronics is located in contact with the heat sink but just outside the rectangular duct. Below the TEG, a NEOCERAM glass of surface area 40x40 mm and 4 mm thickness is included in order to estimate the overall thermal conductance of the TEG following the methodology employed in [3].

The hot side of the NEOCERAM is in contact with an aluminium disc that is being heated by a SELECTA COMBIPLAC electronically controlled heat source. Type K thermocouples ( $\pm 1.5^\circ\text{C}$ ) 0.25 mm thickness are located at the center of the contact surfaces in order to measure temperatures. The thermocouples are inserted in 0.25 mm thin brass sheets in order to assure a good contact between surfaces. The ambient temperature (i.e., the temperature of the incoming air) is also measured with a type K thermocouple. Temperature data are acquired with a NI cDAQ-9174 unit of National Instruments and analysed with LabView software. Open circuit voltage and intensity of the TEG are also monitored with the same NI unit but with different modules. The air pressure loss across the heat sink is acquired by means of a SENSIRION SDP610-125 PA differential pressure sensor ( $\pm(0.1+3\%)$ Pa) connected to a junction of three probes located 10 mm upstream and 10 mm downstream of the heat sink. The flow velocity in the 40x40 cross-sectional rectangular duct is measured with a hot-wire anemometer VELOPORT 2.0 ( $\pm(0.04+1\%)$ m s<sup>-1</sup>) averaging data obtained after inserting the probe at five different depths.

Experimental data is obtained by adjusting the heating plate in order to obtain a hot side temperature of the thermoelectric module equal to 250 °C for any air velocity.



Fig. 2. Finned heat sink tested and employed for validating the model.

### 3. Model set up

The simulation model is based on ANSYS-CFX, a multi-physics commercial software widely employed in the simulations of heat transfer processes between flows and solids.

Here we have modelled the entire rectangular duct, meshing the solid parts with hexahedrons and the fluid region with triangles at the surface, two layer of prisms attached to the surfaces and tetrahedrons in the rest of the fluid volume. A refined region with characteristic element size equal to 0.5 mm has been used closed to the heat sink, whose element size is 1 mm. Other domains of the model

use 2 mm as a characteristic element size. The mesh uses a total number of  $1.39 \times 10^6$  elements (Fig. 3).

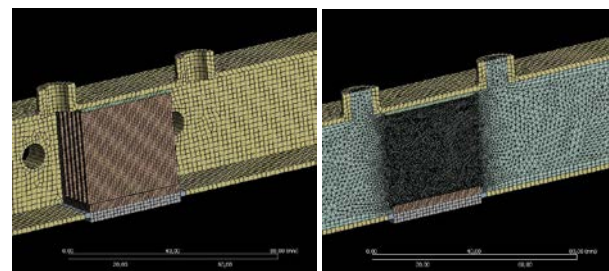


Fig. 3. Detail of the mesh of solid elements (left) and air (right) used in the model.

The boundary conditions are wall in all surfaces except at the duct inlet (with a constant velocity and temperature of the incoming flow) and at the duct outlet (atmospheric pressure). The model includes the definition of all materials involved in the system, whose properties are needed for correctly reproducing the heat transfer (densities, thermal conductivities, wall roughness). For the TEG, we have simulated it as a solid element with a thermal conductance obtained from the measurements and using the methodology explained in [3]. The steady state simulations applies a criterion of residuals equal to  $10^{-4}$  for all variables. The flow is assumed turbulent for cases with mean air velocities above 0.75 m s<sup>-1</sup> since at that velocity the Reynolds number coincides with the critical one for square ducts ( $= 1673$ ) [4]. The heat flux in the near-wall region is modelled using a scalable wall function approach that takes into account the Prandtl number and the surface roughness (see [5] for details). Since the heat transfer is entirely modelled by the finite element method applied to solids and fluids, the fin efficiency and effectiveness factors are not explicitly required.

### 4. Model validation

The ANSYS-CFX model is validated by comparison with experimental data. Figure 4 shows both laboratory and simulated results of the pressure losses through the heat sink. The model agrees with data (within the uncertainty range) for mean flow velocities in the rectangular duct greater than 1 m s<sup>-1</sup>.

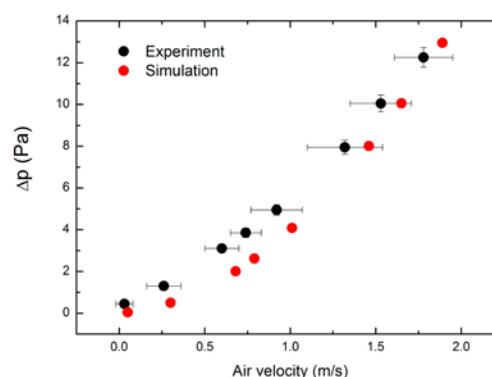


Fig. 4. Experimental and simulated pressure losses  $\Delta p$  through the heat sink as a function of the mean air flow velocity in the cooling rectangular duct.

On the other hand, the prediction of the temperature difference across the TEG also agrees well with the experimental results (see Fig. 5). The main discrepancies appear at low air flow velocities, which indicates that some heat losses, dominant at low flow rates, may not be accurately included in the model (for example, radiation losses in the rectangular pipe to the ambient). The discrepancy at low velocities may be also due to the assumption of a laminar flow (cases with  $v < 0.75 \text{ m s}^{-1}$ ) that may not occur in the actual system due to surface roughness and uneven duct surfaces. However, these low velocity regions are not relevant in our study, since the maximum power is always achieved at higher regimes. Therefore, the results from the CFD model can be used for predicting the output power of the TEG module when using forced convection air cooled finned heat sinks.

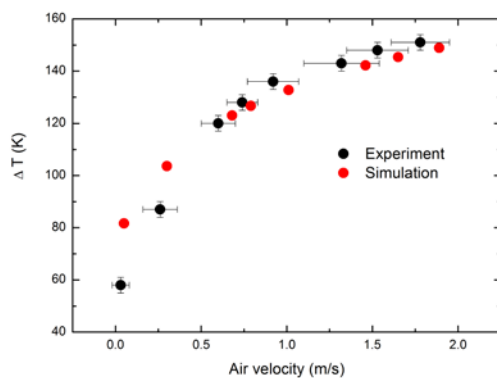


Fig. 5. Experimental and simulated temperature differences  $\Delta T$  at cold and hot TEG sides as a function of the mean air flow velocity in the cooling rectangular duct. The hot TEG side temperature is kept at  $250^\circ\text{C}$  in all cases.

## 5. Results and discussion

The effect of using different type of heat sinks on the performance of the TEG is investigated by simulating 12 different geometries. Table I lists the number of fins, the fin thickness and the fin to fin distance for all cases analysed. All the heat sinks have the same base surface area ( $40 \times 40 \text{ mm}$ ) and fin heights ( $29.5 \text{ mm}$ ). In table I, the total exchange area of the heat sink in contact with the air is also shown for each case.

Table I. Main characteristics of the heat sinks analysed.

NUMBER OF FINS	FIN THICKNESS (mm)	FIN SPACING (mm)	HEAT SINK EXCHANGE AREA ( $\text{cm}^2$ )
9	1	3	228.4
9	1	3.67	228.4
9	1.5	2.8	228.4
10	1	3	252.0
11	1.5	2	275.6
11	1.5	2.2	275.6
12	1	2.6	299.2
12	1.5	2.1	299.2
14	1	2	346.4
14	1.5	1.5	346.4
16	1	1.65	393.6
16	1.5	1.1	393.6

Simulations fix a temperature at the hot side of the TEG equal to  $250^\circ\text{C}$ , which is the temperature of the module expected to give the highest performance. The maximum electrical output power is predicted from the temperature difference across the TEG module  $\Delta T$  by means of

$$P_{\text{TEG}} = a\Delta T + b\Delta T^2 \quad (1)$$

where  $a = -2.994 \times 10^{-3} \text{ K}^{-1}$  and  $b = 1.205 \times 10^{-4} \text{ K}^{-2}$ . Equation (1) has experimentally been obtained with the TEG module used in our study when fixing the hot side temperature of the TEG at  $250^\circ\text{C}$ , cooling down the cold side at different temperatures and, for each  $\Delta T$ , varying an external load resistance in order to extract the maximum output power. The correlation coefficient of this fit is equal to  $R^2 = 0.998$ .

The power of the fan required for moving the air through the heat sink only is calculated as

$$P_{\text{fan}} = \frac{Q\Delta p}{\eta_{\text{fan}}} \quad (2)$$

where  $Q$  is the volumetric flow,  $\Delta p$  the pressure difference across the heat sink and  $\eta_{\text{fan}}$  is the fan efficiency (here assumed to be 0.6).

The net power is

$$P_{\text{net}} = P_{\text{TEG}} - P_{\text{fan}} \quad (3)$$

and represents the available electrical power of the whole TEG system (TEG generation minus consumption by the fan).

Figure 6 shows an example of the results obtained for the heat sink with 12 number of fins 1.5 mm thick. As expected the power required by the fan increases non-linearly as a function of the air flow. On the other hand, the TEG output power shows a monotonic increase as a function of the air velocity  $v$  due to the enhancement in the heat transfer from the heat sink to the flow. For example, at  $v = 5 \text{ m s}^{-1}$ , the temperature difference across the TEG module reaches  $\Delta T = 168^\circ\text{C}$  whereas at  $v = 2 \text{ m s}^{-1}$ ,  $\Delta T = 141^\circ\text{C}$ . The net power of the whole TEG system reaches a maximum at intermediate fluid flow velocities.

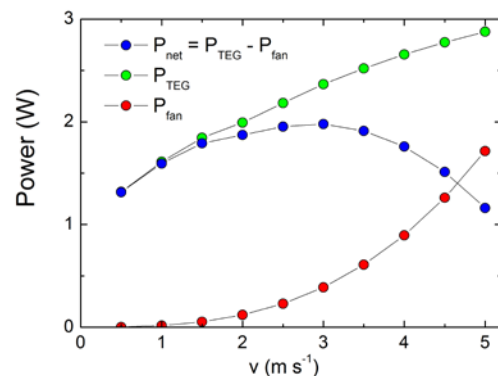


Fig. 6. TEG power ( $P_{\text{TEG}}$ ), fan power  $P_{\text{fan}}$  for moving the air through the heat sink, and net power as a function of the mean air velocity  $v$  (case: heat sink with 12 fins 1.5 mm thick).

The maximum net power obtained for each one of the 12 heat sinks analysed is shown in Fig. 7 as a function of the

heat sink exchange area  $S$ . Data are obtained after fitting a second order polynomial fit to  $P_{net}$ . For example, for the case shown in Fig. 6,  $P_{net,max} = 1.99$  W for  $v = 2.67$  m s<sup>-1</sup>.

As expected, the maximum net output power increases with  $S$ . For a fixed heat sink exchange area  $S$  (i.e., same number of fins), the heat sinks with thicker fins correspond to those with the highest net power. Since the number of fins and the base area are the same, an increase in the fins thickness leads to small gaps between them (smaller fin to fin distances, see Table I). This reduction in cross-sectional area increases the air velocity, thereby enhancing the heat transfer in comparison with heat sinks with larger fin to fin distances. The improvement in the heat transfer leads to a better performance of the TEG.

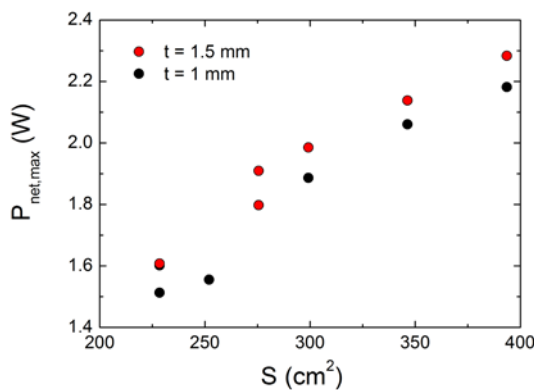


Fig. 7. Maximum net power as a function of the heat sink exchange area for the cases listed in Table I ( $t$  = fin thickness).

However, an increase in the air flow velocity that circulates through the fins also implies an increase in the pressure head losses. This effect reduces the net power since it increases the fan power requirements. All in all, the overall effect of increasing the fin thickness, with the same value of the heat sink exchange area, is to increase the net power output that is reached at lower fluid flow velocities.

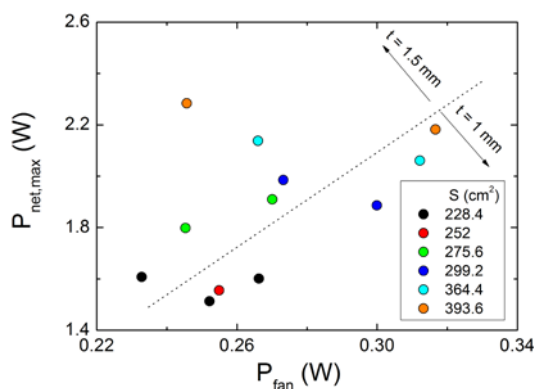


Fig. 8. Maximum net power as a function of the fan power requirement ( $t$  = fin thickness;  $S$  = exchange surface area of the heat sink).

Figure 8 shows the maximum net power output as a function of the fan power, the latter being proportional to  $v^3$ . For clarity, the exchange surface area  $S$  for each case is also shown. Results can be clearly divided into two regions depending on the fin thickness  $t$ . Higher values of fin

thickness generate more net power with low fan power requirements.

The increase in the performance of thicker fins may lead to values of net output power similar to those obtained with heat sinks with more but thinner fins (compare, e.g., case  $S = 364.4$  cm<sup>2</sup> and  $t = 1.5$  mm with case  $S = 393.6$  cm<sup>2</sup> and  $t = 1$  mm in Fig. 8). In addition, heat sinks with thicker fins have the advantage of requiring less fan power for reaching the maximum output point. This may lead to more economical fan devices and, consequently, more economical TEG systems.

## 6. Conclusions

The effect of changing the geometry of air cooled finned heat sinks on the performance of a TEG system has been analysed. Experimental data obtained in the laboratory have been used for validating a numerical model. The model uses ANSYS-CFX and includes heat transfer mechanisms between solid and fluid regions. The TEG has been modelled as a solid element whose transport coefficients are determined following the methodology found in [3].

Simulations of several heat sinks are performed in order to evaluate the available net power (TEG production minus fan consumption). The results indicate that: 1) the TEG performance improves when increasing the exchange surface area of the heat sink (as expected) and 2) for a fixed exchange surface area, thicker fins provide better results since generate more net power with low fan power.

This last result implies that economical extrusion-based aluminium heat sinks are very good options for air cooled finned heat sinks in TEG applications.

## Acknowledgement

This work has been partially funded by the University of Girona under grant MPCUdG2016-4. Sergi Saus and Jordi Vicens provided very helpful technical assistance.

## References

- [1] E. Massaguer, A. Massaguer, T. Pujol, J.R. Gonzalez, L. Montoro, "Modelling and analysis of longitudinal thermoelectric energy harvesters considering series-parallel interconnection effect", in *Energy*, 2017, Vol. 129, pp. 59-69.
- [2] M. Karvonen, R. Kapoor, A. Uusitalo, V. Ojanen, "Technology competition in the internal combustion engine waste heat recovery: a patent landscape analysis", in *Journal of Cleaner Production*, 2016, Vol. 112, pp. 3735-3743.
- [3] I. Ruiz, M. Borrelli, T. Pujol, N. Luo, L. Pacheco, A. Massaguer, L. Montoro, "Effective thermal conductance of thermoelectric generator modules", in *Renewable Energy and Power Quality Journal*, 2017, Vol. 1, pp. 545-550.
- [4] I. Tosun, D. Uner and C Ozgen, "Critical Reynolds number for newtonian flow in rectangular ducts", in *Industrial and Engineering Chemistry Research*, 1988, Vol. 27, pp. 1955-1957.
- [5] ANSYS-CFX Solver Theory Guide. ANSYS, Inc, 2015.